EFFECT OF FLUXING ADDITIVES IN FERRIMAGNETIC FRITS OF THE Fe-Si-Ca-Al SYSTEM

Rosales-Sosa Gustavo Alberto, [1] Poirier Thierry, [1] Joaquín Lira-Olivares, [2] Carda-Castello Juan Bautista

Department of Materials Sciences,
Universidad Simón Bolívar, AA89000, Caracas 1080A, Venezuela.
tpoirier@usb.ve

Department of Inorganic and Organic Chemistry,
Universidad Jaume I, Castellón, Spain.
carda@qio.uji.es

ABSTRACT

Glasses rich in transition oxides, particularly with iron oxide, have been studied for their interesting properties such as: semi-conductivity, ferrimagnetism, and chemical stability, among others. Frits in the Fe-Si-Ca oxide system are potentially useful for use in conductive glazes or as electromagnetic wave-absorbing aggregates, but their properties could be improved. In this sense, the effect of different additives such as Li_2O and B_2O_3 was studied with a view to enhancing the fusibility and improving the magnetic and conductive properties of the material in frits with 30–40% Fe_2O_3. The frits were prepared in silico-aluminous crucibles and characterised by X-ray diffraction (XRD), scanning electron microscopy (SEM), and differential thermal analysis and thermogravimetry (DTA–TG). The formation of crystalline magnetite dendrites was confirmed in frits with 40% Fe_2O_3. The effect is discussed of the atmosphere and working temperature of the crucible furnace and of the oxide additives on the phases present and on their ferrimagnetic performance. Finally, the frits were applied as glaze compositions to evaluate their ability to adapt to the floor and wall tile production process: maturing defects were detected concomitant with the presence of Anorthite and Hematite phases, which suggest the importance of the fusion conditions and the greater interaction between the silico-aluminous crucible and the frits with more fusible additives.

1. INTRODUCTION

Glasses that are rich in transition metals, such as iron, are of considerable interest in medicine, electro-ceramics, optical ceramics, structural ceramics, and waste sectors, as well as in geology and the basic sciences. In particular, iron oxide-rich glasses are well known for their conductive and ferromagnetic properties, bioactivity, biocompatibility, and chemical stability, whose presence depends on the composition and on the synthesis method and subsequent thermal treatments.[1-9]

In the building sector, and in particular in floor and wall tile manufacturing, iron oxide-rich glasses have been used for the development of glazes with metallic effects, using compositions rich in P_2O_5 and Fe_2O_3.[10,11] The wide range of properties that such glasses display provides then with great potential in the development of numerous technological applications. One such application is the development of semiconducting glazes for antistatic or radiant flooring. Semiconducting glazes have been successfully developed in the systems SnO_2-Sb_2O_5 and TiO_2-Nb_2O_5.[12,13] In particular, glazes have been developed in the system SnO_2-Sb_2O_5 for heating applications (heating by the Joule effect).[14]

In addition, iron oxide-rich semiconducting glazes have been developed for porcelain electric insulators.[15,16] In these glaze compositions, a mixture of conventional transparent frit and different metallic oxides (Fe_2O_3, NiO, ZnO, CoO, Cr_2O_3, CuO, and TiO_2) are used, which are subjected to a thermal treatment that results in the formation of magnetite (Fe_3O_4). The (semiconducting) magnetite in these glazes forms conduction paths that provide the glaze with its semiconducting character, as well as its heating capability. Particularly to be noted is the semiconducting character of Fe_3O_4, which conducts electrons by polaron conduction: electron transfer between Fe^{2+} and Fe^{3+}.[17]

A system of interest is SiO_2-CaO-Fe_2O_3. This system was initially studied for its magnetic properties and subsequently for its biomedical applications. In numerous studies this system has shown an ability to vitrify or form high-temperature eutectics, and to crystallise phases such as β-CaO.SiO_2 (Wollastonite), zinc ferrites, magnesium ferrites, apatite in magnetic clusters, magnetite (Fe_3O_4) and γ-Fe_2O_3, Hematite (Fe_2O_3), and cristobalite.[1,6,7,8,9]

In seeking to obtain semi-conductivity in floor tile glazes, taking advantage of magnetite's ease of crystallisation in systems rich in iron oxides, previous studies developed glazes in the chemical system SiO_2-CaO-Fe_2O_3, which could be adapted to the ceramic floor and wall tile production process.[18,19] However, the magnetic and conductive properties could be enhanced. The addition of fluxes to these systems would allow the melting temperatures of these materials to be lowered and could improve their ferrimagnetic properties. Additives such as Li_2O and B_2O_3 are good candidates for frit improvement.[20-23] On the other hand, the Fe^{2+}/Fe3+ proportion could influence magnetite conductivity and quantity. On the basis of the interesting results obtained previously and the motivations for this study, the following objectives were considered:

- On the basis of the compositions developed in previous studies, to synthesise ferrimagnetic compositions in the system Fe-Si-Ca, at the same time studying the effect of additives such as Li_2O and B_2O_3.
- To study the effect of the atmosphere and melting temperature on the frits being studied.
- To study the adaptability of the frits to the floor tile production process with potential technological applications.

2. EXPERIMENTAL

2.1. Synthesis of frits and glazes

The frits in this study are based on compositions of foregoing studies[18,19], which are iron oxide-rich silica glasses that start from the ternary phase diagram SiO_2-CaO-Fe_2O_3. The present study examines the effect of the addition of Li_2O and B_2O_3 and the effect of fusion conditions on the original compositions. The frits were synthesised by direct fusion in laboratory crucible furnaces at temperatures of 1400 °C for one hour. For this, industrial raw materials and silico-aluminous crucibles were used. Frits were also synthesised in gas furnaces at 1300 °C for one hour in silico-aluminous crucibles. It should be noted that in general the fusion environment of gas furnaces is more oxidising than that of electric furnaces (which are usually neutral to slightly oxidising). The compositions of the study are detailed in Table 1.

	Composition (% by weight)				
Frit	**SiO_2**	**CaO**	**Li_2O**	**B_2O_3**	**Fe_2O_3**
1	45	25	-	-	30
2	40	20	-	-	40
3	45	21	4	-	30
4	40	16,8	3,2	-	40
5	40	25	-	5	30
6	35,6	20	-	4,4	40

Table 1. Compositions of the iron oxide-rich frits of the present study.

The raw materials (of an industrial nature): SiO_2, $CaCO_3$, Fe_2O_3, Li_2CO_3, and H_3BO_3, were mixed by hand in the appropriate proportions, and then fused and quenched in water according to the conventional fritting process. The aluminium oxide subsequently present in the test frits came from the crucibles, which were highly corroded during fusion. Glazes were then obtained by mixing the frits with CMC, sodium tripolyphosphate (TPP), kaolin (10%) and sufficient water to obtain a fluid suspension. The resulting suspensions were applied on porcelain tile subs-

trates, which were dried and fired at 1200 °C in a pilot kiln of an industrial type fuelled by natural gas.

2.2. Characterisation techniques used

The quantitative chemical analysis of the frits obtained was performed in an X-ray fluorescence instrument (Bruker AXS S4 Pioneer). The thermal stability and physico-chemical changes of the studied frits were assessed by differential thermal analysis and thermogravimetry (DTA-TG: Mettler Toledo TGA/SDTA851, from 25 to 1200 °C, 10 °C/min). The crystalline phases in the frits and in the resulting glazes were determined by means of an X-ray diffractometer (XRD: Bruker D4 ENDEAVOR with copper anode, 20mA, 40 KV, 10–80°). The characteristic temperatures of the frits fused at 1400 °C were determined with a Misura 3.32 hot stage microscope (600–1400 °C, 20 °C/min). The dilatometric coefficients of the frits fused at 1400 °C were determined using a Bahr Thermo Analyse DIL 80I L differential dilatometer (5°C/min, from 25 °C to the softening temperature of each frit). The microstructural characterisation of the frits and glazes was carried out by scanning electron microscopy (JEOL JSM 6390 and HITACHI S-2400, 25KV).

3. RESULTS AND DISCUSSION

3.1. Characterisation of the frits

Tables 2 and 3 present the chemical analyses of the frits fused in the gas crucible furnace at 1300 °C and in the electric furnace at 1400 °C, respectively.

	Composition (% by weight)						
Sample	**SiO_2**	**CaO**	**Fe_2O_3**	**Al_2O_3**	**Li_2O**	**B_2O_3**	**Other oxides**
1	44,10	25,90	29,40	0,80	-	-	0,20
2	39,75	21,10	37,80	1,10	-	-	0,20
3	44,35	21,75	29,15	1,50	?	-	0,30
4	40,50	17,90	37,80	1,20	?	-	0,20
5	40,65	26,15	29,05	1,40	-	?	0,30
6	36,25	21,25	38,00	0,90	-	?	0,10

Table 2. XRF chemical analysis in % by weight of the frits fused in the gas crucible furnace at 1300 °C. (?) Li_2O and B_2O_3 were not quantified by XRF.

	Composition (% by weight)						
Sample	**SiO_2**	**CaO**	**Fe_2O_3**	**Al_2O_3**	**Li_2O**	**B_2O_3**	**Other oxides**
1	43,35	20	23,35	13,70	-	-	0,58
2	39,45	15,65	30,80	14,45	-	-	0,64
3	43,40	17,35	25,15	11,75	?	-	0,55
4	39,80	13,70	33,10	11,35	?	-	0,59
5	39,55	18,75	22,25	16,25	-	?	0,65
6	37,65	15,80	30,15	13,20	-	?	0,60

Table 3. XRF chemical analysis in % by weight of the frits fused in the electric laboratory crucible furnace at 1400 °C. (?) Li_2O and B_2O_3 were not quantified by XRF.

The above tables show that, for both frits, a strong deviation was generated in the composition independently of the temperature or fusion atmosphere. It is evident that, at a higher melting temperature, the frit was more corrosive, evidenced by the high quantity of alumina in the frits synthesised at 1400 °C (up to 16.25% by weight compared with 1.5% at 1300 °C) and by the deviation of the values of CaO. The percentage of silicon was not strongly affected, possibly due to the dissolution of SiO_2 from the silico-aluminous crucible. A greater content of oxides foreign to the composition was also observed. Figure 1 shows the diffractograms of the frits fused at 1300 °C in the gas furnace and at 1400 °C in the electric furnace, respectively.

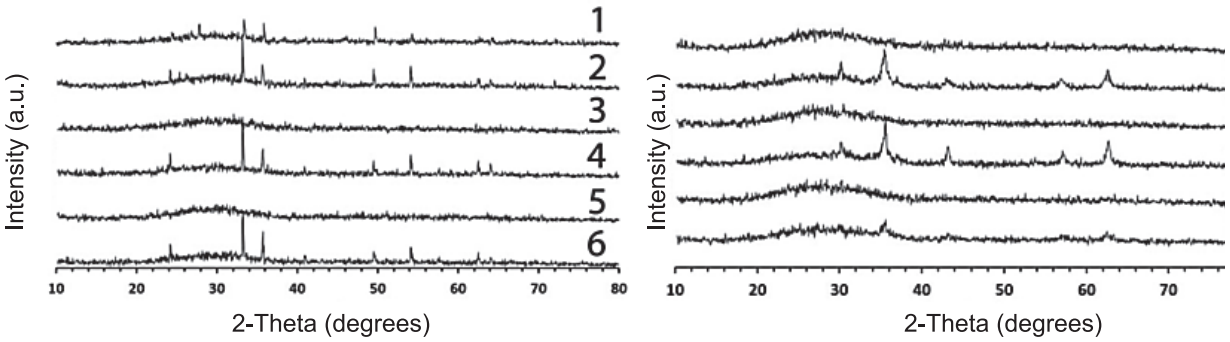

Figure 1. XRD spectrum of the frits fused at **1300 °C** *(left). The only phase present is Hematite (Fe_2O_3). Crystallographic files: 01-089-8104 (C) – Hematite, 01-089-7047 (C) Iron Oxide and 01-089-0599 (C) – Hematite,*

(contd.) XRD spectrum of the frits fused in the electric furnace at **1400 °C** *(right). The only phase present is Magnetite (Fe_3O_4). Crystallographic files: 03-065-3107 (C) – Iron Oxide – Fe_3O_4 and 01-089-0950 (C) – Magnetite – Fe_3O_4.*

The frits obtained at 1300 °C exhibited a crystalline character in most of the samples, Hematite (Fe_2O_3) being the primary crystalline phase. Results obtained by SEM, not shown in this paper, confirmed the presence of crystallised Hematite during cooling which was not dissolved in the glassy matrix, possibly due to the low

working temperatures (below the eutectic point according to the SiO_2-CaO-Fe_2O_3 ternary diagram).[18] Similarly, it should be noted that the addition of oxide fluxes limited the appearance of crystalline phases in samples 1, 3, and 5 (with lower Hematite content) synthesised at 1300 °C and at 1400 °C.

For the frits obtained at 1400 °C, the presence was observed of Magnetite in samples 2, 4, and 6 (designed with 40% Fe_2O_3), sample 6 being the least crystalline. This is understandable since B_2O_3 is a glass network former.[20] In this regard, the effect of fusion atmosphere and temperature may be observed: higher temperatures and lower oxygen partial pressure during fusion favour the reduction of Hematite (passing from Fe^{+3} to Fe^{2+} as the Ellingham diagram suggests) and its entry into the glass network.[18] The partial reduction of Fe^{+3} to Fe^{+2} favours subsequent Magnetite nucleation (Fe_3O_4) in the glass, which is a phase of the spinel type with simultaneous states of Fe^{+2} and Fe^{+3} ($FeO{\cdot}Fe_2O_3$).[17]

In the rest of the paper, only the results of the frits synthesised at 1400 °C are presented, owing to their ferromagnetic and semiconducting properties of interest. Figure 2 shows images of the frits synthesised at 1400 °C, obtained by scanning electron microscopy.

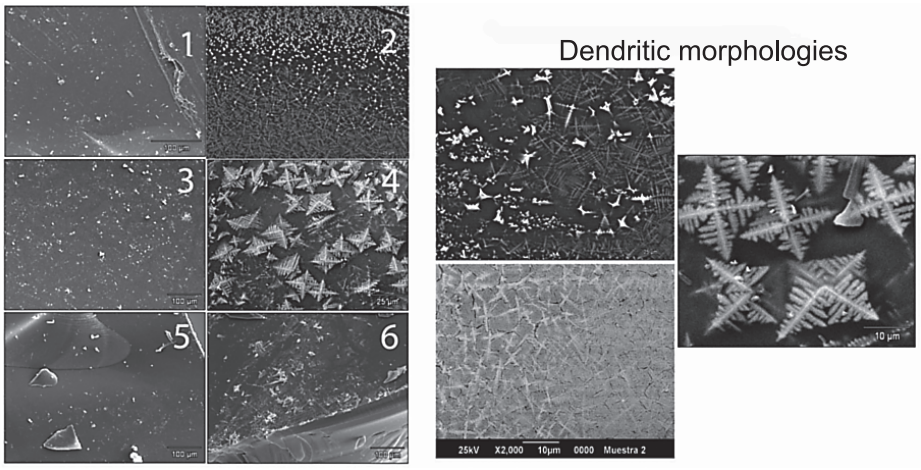

Figure 2. SEM micrographs in the backscattered electron mode of the frits fused at 1400 °C and three micrographs (right) displaying different dendritic morphologies found in frits 2 and 4.

The SEM micrographs show that magnetite dendrites were only observed in the frits with a greater iron content (2 and 4). Even though frit 6 contained magnetite, as the diffraction results suggested, it was not possible to observe this by SEM. This could be related to the low crystallinity observed by XRD. The magnetite in systems rich in iron silicates usually crystallises with a dendritic morphology when they are rapidly cooled.[25-26] It may be noted that samples 2, 4, and 6 responded strongly to the presence of a magnet. The characteristic temperatures and coefficients of experimental and theoretical linear thermal expansion (Appen) for the frits synthesised at 1400 °C are detailed in Table 4.

	Characteristic points		α (10^{-7} 1/K)[1]		α(10^{-7} 1/K)[2]
Samples	T_g	T_a	50 °C-300°C	300 °C-500 °C	20 °C – 400 °C
1	771	908	68,8	76,8	58,1
2	707	1123	62,5	68,7	54,2
3	621	1103	53,8	62,4	56-7 - 76,4
4	620	1051	58,1	66,2	53,9–71,2
5	653	1016	58,3	69,5	56,3–50,8
6	681	1000	64,6	74,8	55,5–50,3

Table 4. Characteristic points (T_g - glass transition temperature and T_a - dilatometric softening temperature) and linear dilatometric coefficients (α) of the studied frits [1]. Range of linear dilatometric coefficients (α) determined by Appen's formula [2], in a range of values of Li_2O and B_2O_3 located between 0 and the design percentage.

The fluxing oxide addition to the composition reduced the frit T_g. However, the softening temperature was generally observed to rise. The increase in softening temperature could be due to the appearance of crystalline phases during thermal treatment, which could slow down the detection of the glass softening point.

With relation to the dilatometric coefficients, it was observed that both additives reduced these coefficients, this effect being more pronounced for Li_2O. A reduction of α was to be expected with the addition of Li_2O (network modifier).[22] The contamination by Al_2O_3 as a result of the attack on the crucibles undoubtedly affected the new value of α, and tended to reduce expansion, but the paradoxical difference between the measured values and the values determined by Appen's theoretical calculation (which included the effect of Al_2O_3), may be explained more satisfactorily by the presence in the glassy matrix of crystalline phases, still in incipient quantities: for example, from lithium (β-Spodumene, Virgilite), hardly detectable by XRD below a certain quantity (2–3%). These phases are well known for their low dilatometric coefficients. A small fraction could contribute adversely to the overall dilatometric coefficient. In the case of B_2O_3, a slight decrease in the dilatometric coefficient was also observed at 30% Fe_2O_3, but an increase was observed at 40%. Compared with the Appen calculations, this effect again suggests an alteration of α by crystal formation in the glassy matrix.

This difference between the experimental value for the dilatometric coefficient and the one calculated by Appen's equation was verified to be a tool in confirming the glass-ceramic character of a frit[26]. The sintering curves of the studied frits are plotted in Figure 3.

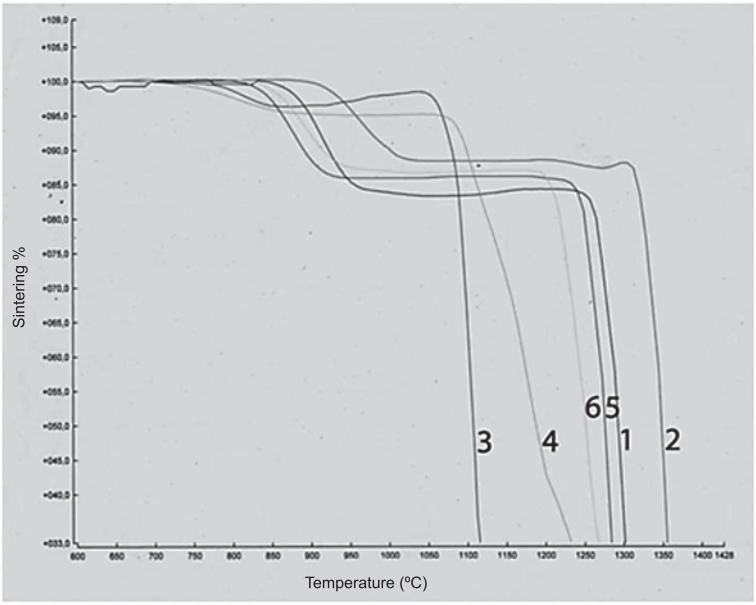

Figure 3. Sintering curves of the frits fused at 1400 °C, determined by hot stage microscopy.

The sintering curves of the samples again reveal the fluxing effect of the additives in the samples. In general, when the Fe_2O_3 contents increased, the melting temperatures of the material increased. This effect was reversed in the case of the samples with B_2O_3, albeit with very little difference. On the other hand, it was observed that sintering started in all samples in a range of 700 to 900 °C and they sintered fully in a range between about 850 and 1100 °C.

Figure 4 shows the differential thermal and thermogravimetric analysis curves of the frits fused at 1400 °C, which help anticipate their behaviour in fused glazes on tiles.

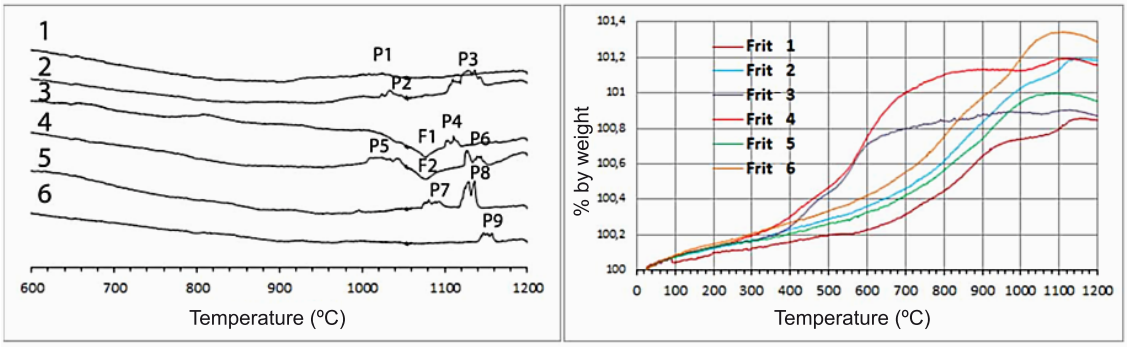

Figure 4. Differential thermal and thermogravimetric analysis curves of the frits fused at 1400 ºC in air.

According to the DTA curves, all samples appeared to exhibit crystallisation peaks. All samples crystallised strongly around 1100–1150 °C (P1, P3, P4, P6, P7, P8, and P9) and incipient crystallisation occurred for frits 2, 4, and 7 (P2, P5, and

peak near 1000 °C for sample 5). Finally, a pronounced fusion was observed for the frits with Li_2O (about 1080 °C). Most crystallisation phenomena appeared to be complex in nature in view of the number of crystallisation peaks.

The thermogravimetric curves associated with the DTA indicated that all samples underwent oxidation for all compositions. It was observed that the samples with Li_2O oxidised more rapidly than the other frits. This is reasonable, considering that the glass with Li_2O has a more open structure, which is more susceptible to atomic diffusion. Finally, samples 1, 3, and 5 gain a maximum of 0.8–1% by weight, whereas samples 2, 4, and 6 gain about 1.2–1.35% by weight.

3.2. Characterisation of the obtained glazes

The XRD spectra of the studied samples are shown in Figure 5.

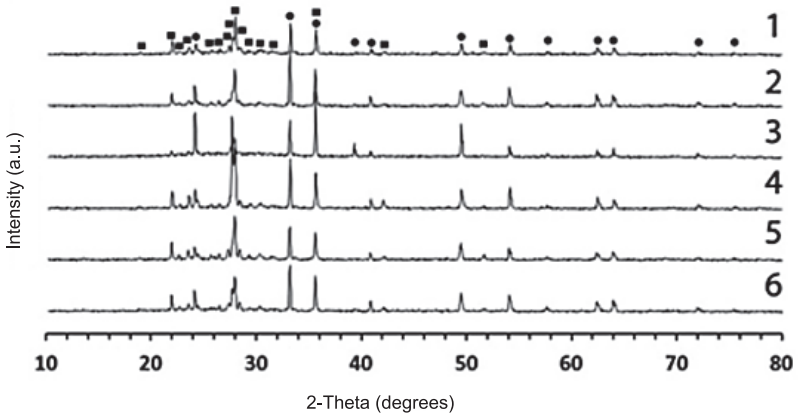

Figure 5. XRD Spectra of the glazes obtained by fusion at 1400 °C. • Hematite (Fe_2O_3), ■ Anorthite ($CaAl_2Si_2O_8$). Crystallographic files 411486 (PDF2) – Hematite – alpha-Fe_2O_3 and 01-089-1477 (C) – Anorthite, Annealed – (Ca0.98Na0.02)(Al1.98Si0.02)Si2O8).

The XRD spectra in the figure show that the predominant crystalline phases in the glazes were Hematite and Anorthite. Hematite had already been encountered in previous studies with similar compositions, and its formation seemed to arise with the gain in weight seen in TG: the oxidation of frit Magnetite takes place in the kiln in glazed tile production. Unfortunately, the addition of Li or B to the frit did not avoid this phenomenon. The presence of Anorthite is explained by the high values of alumina originating from the fusion crucible and the kaolin from the glaze composition.

The micrographs of the cross-sections and surfaces of the glazes are shown in Figure 6. An image is also presented of the surface of sample 4, which clearly shows Anorthite and Hematite crystals.

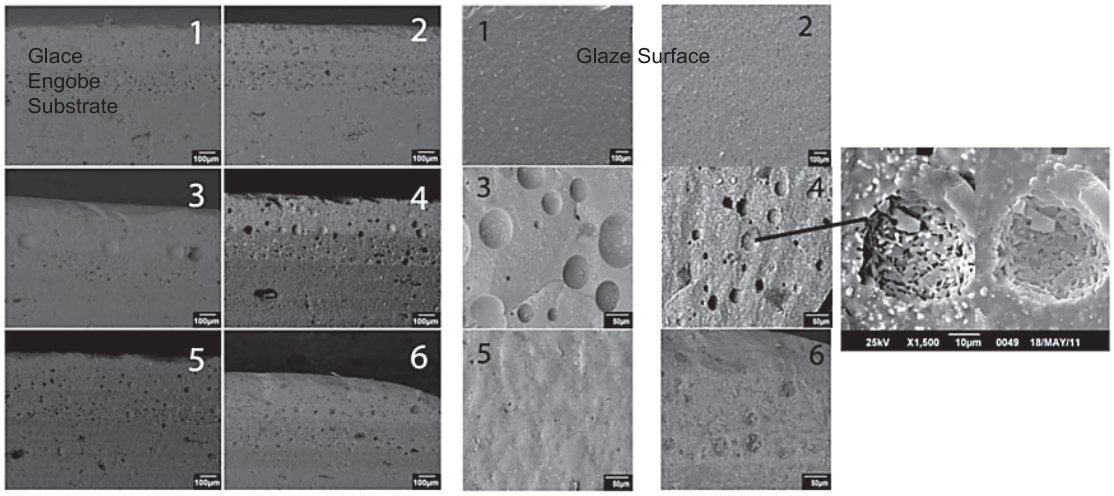

Figure 6. SEM micrographs of cross-sections and surfaces of the test glazes and an image of the surface of sample 4 (right, showing Anorthite crystals (angular grey crystals) and Hematite crystals (white crystals).

Most of the coatings exhibited porosity in the engobe and in the glaze, which is unfavourable for ceramic products. Similarly, the porosity present was observed at the surface and in the subsurface. It may be noted that the porosities increased in the glaze compositions with frits whose TG curve displayed a greater mass loss above 1100 °C. An incipient reduction in hematite in this range would then appear likely. The largest surface pores were observed in the samples containing Li_2O as additive, which usually suggests greater flowability of the molten glazes.

4. CONCLUSIONS

Ferrimagnetic frits were obtained in the system Fe-Si-Ca-Al for compositions of about 30% by weight of Fe_2O_3, which exhibited magnetite of dendritic morphology as primary crystalline phase, this effect being more pronounced for frits without additives and with Li_2O. The appearance of magnetite in the frits was only favoured at high temperatures and in atmospheres between neutral and slightly oxidising. Lithium oxide had a strong fluxing effect and increased the oxidation kinetics of the frits compared to the frits without additives. To be noted was a greater attack on the crucible and the subsequent contribution of alumina to the material, which, however, did not prevent magnetite formation. The absence of magnetite in the glazes indicates that the fabrication of magnetite-rich semiconducting glazes requires modifying the firing cycle atmosphere to less oxidising conditions, while concurrently attempting to increase the percentage of Fe_2O_3 in the compositions. If this constraining technology is not upgraded, the use of frits with the addition of lithium as fillers for the absorption of high-frequency electromagnetic radiation remains interesting. In contrast, boron contributes satisfactorily to the creation of magnetite. In a future study, it is expected magnetically and electrically to characterise the frits obtained in this work.

ACKNOWLEDGEMENTS

The authors thank the staff of the Servei Central d'Instrumentació científica of Universidad Jaume I of Castellón for their continuous support and shared technical knowledge.

REFERENCES

[1] KAWASHITA. M, International of Applied Ceramic Technology, Vol. 2, (2005), pp. 173-183.

[2] EL-DESOKY. M.M, IBRAHIM. F.A, MOSTAFA. A.G, HASSAN. M.Y, Materials Research Bulletin, Vol. 45, (2010), pp.1122-1126.

[3] ROMERO. M.P, RINCON. J. MA, GONZALEZ-OLIVER. C.J.R, D'OVIDIO. C, ESPARZA. D, Materials Research Bulletin, Vol. 36, (2011), pp. 1513-1520.

[4] HANNANT. O.M, FORDER, S.D, BINGHAM, P.A, HAND. R.J, Hyperfine Interactions, Vol. 192, (2009), pp. 34-42.

[5] COCHAIN. B, NEUVILLE. D.R, DE LIGNY. D, ROUX. J, BAUDELET. F, STRUKELJ. E, RICHET. P, Jounal of Physiscs: Conference Series, Vol. 190, (2009), pp.1-5.

[6] POIRIER. T, LABRADOR. N, ÁLVAREZ. M.A, LAVELLE. C, ENET. N, LIRA. Materials Letters, Vol. 59, (2005), pp. 308-312.

[7] HAYASHI. M, SUSA. M, MARUYAMA. T, NAGATA. K, Journal of Electronic Materials, Vol. 24, (1995), pp. 983-989.

[8] SINGH. K.R, SRINIVASAN. A, Journal of Magnetism and Magnetic Materials, Vol. 323, (2011), pp. 330-333.

[9] DA LI. G, DA LI. Z, LIN. Y, HUA PAN. T, SHENG CHEN. G, DAN YIN. Q, Materials Science and Engineering C, Vol. 30, (2010), pp. 148-153.

[10] ES-Pat. 2 161 193 A1 (2001).

[11] ES-Pat. 2 161 193 B1 (2002).

[12] TAYLOR. R.H,Journal of Materials Science, Vol. 12, (1977), pp. pp. 873-883.

[13] ANGHERA. J.S, WILLIAMSON. J,Journal of Materials Science, Vol. 20, (1985), pp. 4045-4049.

[14] NÚÑEZ. I, GOMEZ. J.J, JOVANI. M.A, GOYENECHE. I, NEBOT. A, CORDONCILLO. E., CARDA. J.B, Key Engineering Materials, Vol. 264-268 (II), (2004), pp. 1369-1372.

[15] FORREST. J.S, Journal of Scientific Instruments, Vol. 24, (1947), pp. 211-217.

[16] LUCAS. D.H, Journal of Applied Physics, Vol. 3, (1952), pp. 293-296.

[17] AMOROS. J.L, BARBA. A, BELTRAN. V, AICE-ITC Instituto de Tecnología Cerámica, Cap. 3, pp. 156, 1994.

[18] ROSALES. G, CARDA-CASTELLÓ. J.C, POIRIER. T, PASCUAL-COSP. J, LIRA-OLIVARES. J, QUALICER, Bloque C, 2010.

[19] ROSALES. G.A, POIRIER. T, CO-SP. J.P, LIRA-OLIVARES, J. CARDA-CASTELLÓ, J.B, Interceram, Vol.60, (2011), pp. 48-52.

[20] LEVENTURI. TH, KIS. A.C, THOMPSON. J.R, ANDERSON. I.M, Biomaterials, Vol. 26, (2005), pp.4924-4931.

[21] LEMBKE. U, HOELL. A, KRANOLD. R, SCHUPPEL. W, MULLER. R, GOERIGK, GILLES. R, WIEDENMANN. A, Journal of Applied Physics, Vol. 85, (1999), pp.2279-2286.

[22] YET. M.C, BIRNIE. D, KINGERY. D,", MIT Series, Wiley, Cap. 1, pp. 97-91, 1997.

[23] HERBERT. J.M, MOULSON. A.J, "Electroceramics: Materials, Properties, Applications", Wiley, SegundaEdición, Cap. 2, 2003.

[24] ALLIA. P, BRETCANU. O, V. ENRICA, CALEGATO. F, COISSON. M, TIBERTO. P, VINAO. F, SPIZZO. F, TAMISAN. M, Journal of Applied Physics. Vol. 105, (2009), pp.

[25] KARAMANOV. A, PISCIELLA. P, MELINO. M, Journal of the European Ceramic Society, Vol 20, (2000), pp. 2233-2237.

[26] RASTEIRO. M.G, GASSMAN. T, SANTOS. R, Antunes. E, Ceramics International, Vol. 33, (2007), pp.345–354.

[27] CARCELLER. J.V, SOLER. A, NEBOT. A, GARCIA-BELMONTE. G, FABREGAT. A, CARDA. J.B, International Ceramics Journal, Research & Development, (1998), pp. 22-29.